

Diabetes mellitus impacts on expression of DNA mismatch repair protein PMS2 and tumor microenvironment in pancreatic ductal adenocarcinoma

Xuekai Pan^{1,2}, Hiroki Mizukami^{1*} , Yutaro Hara^{1,2}, Takahiro Yamada^{1,2}, Keisuke Yamazaki^{1,2}, Kazuhiro Kudoh¹, Yuki Takeuchi¹, Takanori Sasaki¹, Hanae Kushibiki¹, Akiko Igawa^{1,2}, Kenichi Hakamada²

¹Department of Pathology and Molecular Medicine, Hirosaki University Graduate School of Medicine, Aomori, Japan, and ²Department of Gastroenterological Surgery, Hirosaki University Graduate School of Medicine, Aomori, Japan

Keywords

PMS2, Diabetes mellitus, Pancreatic ductal adenocarcinoma

*Correspondence

Hiroki Mizukami
Tel.: +81-0172-39-5025
Fax: +81-0172-39-5026
E-mail address:
hirokim@hirosaki-u.ac.jp

J Diabetes Investig 2022

doi: 10.1111/jdi.13929

ABSTRACT

Aims/Introduction: The mismatch repair (MMR) protein recognizes DNA replication errors and plays an important role in tumorigenesis, including pancreatic ductal adenocarcinoma (PDAC). Although PMS2, a MMR protein, is degraded under oxidative stress, the effects of diabetes are still unclear. Herein, we focused on whether diabetes affected MMR protein expression in PDAC.

Materials and Methods: Tissues from 61 surgically resected PDAC subjects were clinicopathologically analyzed. Immunohistochemical analysis was performed for MMR protein expression, oxidative stress, and immune cell infiltration. The change of MMR protein expression was assessed in PDAC cell lines under stimulation with 25 mM glucose and 500 μ M palmitic acid. Survival curves were analyzed by the Kaplan–Meier method with the log-rank test.

Results: Diabetes complicated with dyslipidemia significantly decreased the expression of PMS2 in PDAC tissues with an inverse correlation with the degree of oxidative stress. Palmitic acid combined with high glucose induced degradation of PMS2 protein, enhancing oxidative stress *in vitro*. CD8⁺ T-cell infiltration was associated with a short duration of type 2 diabetes (≤ 4 years) and a low expression of PMS2 in PDAC tissues, while CD163⁺ tumor-associated macrophage infiltration was increased with a long duration of diabetes (> 4 years). A short duration of diabetes exhibited a better prognosis than nondiabetic subjects with PDAC ($P < 0.05$), while a long duration of diabetes had a worse prognosis ($P < 0.05$).

Conclusions: The different phases of diabetes have a major impact on PDAC by altering PMS2 expression and the tumor immune microenvironment, which can be targeted by an immune checkpoint inhibitor.

INTRODUCTION

Diabetes mellitus (DM) is correlated with a poor prognosis of patients with pancreatic ductal adenocarcinomas (PDACs). Although there are disparate definitions of long-term diabetes, a significant increase in the overall mortality from PDAC has also been observed in patients with long-term diabetes (≥ 3 to

5 years) through epidemiological studies^{1–3}. The frequency of *CDH1* promoter methylation is increased in PDAC complicated with a long duration of diabetes, while the underlying mechanisms of the effect of different durations of diabetes on PDAC have not been fully clarified¹.

In eukaryotes, the mismatch repair (MMR) pathway recognizes DNA replication errors, thereby playing an important role in maintaining DNA fidelity⁴. Although mismatch

Received 7 June 2022; revised 10 September 2022; accepted 6 October 2022

repair-deficient (dMMR) has a low prevalence in PDAC, it is associated with a longer overall survival because of a markedly higher tumor mutational burden and relatively fewer mutations in conventional pancreatic cancer driver genes such as *KRAS* and *SMAD4*⁵⁻⁷. Downregulation of *MLH1* expression is generally combined with the loss of *PMS2* expression. By comparison, the isolated loss of *PMS2* expression implies the occurrence of a *PMS2* gene mutation⁸. A functional *in vitro* MMR assay demonstrated that a low expression of *PMS2* could also mediate MMR capability, as was shown formerly to be the case with the other MMR genes⁹⁻¹².

A rising level of oxidative stress is one of the initial aberrations in the natural history of diabetes¹³. An article reported that reactive oxygen species (ROS) produced during oxidative stress could inactivate the MMR system, especially *PMS2*¹⁴. Therefore, there could be an association between diabetes and *PMS2* expression in PDAC, while it is not fully elucidated yet.

CD8⁺ T cells are the frontline immune cells for fighting tumor cells in the tumor microenvironment (TME)¹⁵. However, their antitumor properties are impaired by immunosuppressive crosstalk between malignant cells and the TME¹⁶. While abundant CD8⁺ T cells are associated with dMMR¹⁷, whether they are correlated with *PMS2* expression is unknown. Considering the abovementioned factors, we focused on the impacts of *PMS2* expression and immune cells in TME on the prognosis of PDAC complicated with DA.

MATERIALS AND METHODS

Patients and specimens

A total of 61 PDAC patients who underwent surgical resection at Hirosaki University Hospital from 2010 to 2014 were analyzed retrospectively. Major clinical characteristics were obtained from the clinical records. Patients with DA fulfilled the criteria of diabetes proposed by the Japan Diabetes Society¹⁸. The presence of dyslipidemia was defined as a triglyceride (TG) level of > 2.47 mmol/L or total cholesterol (TC) > 3.9 mmol/L or low-density lipoprotein-cholesterol (LDL-c) > 4.2 mmol/L or high-density lipoprotein-cholesterol (HDL-c) < 1.0 mmol/L. Sixty-one cases of PDAC were divided into two groups: 32 cases in the non-DA (NDM) group and 29 cases in the diabetes (DM), which were further divided into 14 cases with short-term diabetes (short-DM) (duration of diabetes ≤ 4 years before the PDAC diagnosis) and 15 cases with long-term diabetes (long-DM) (duration > 4 years before the PDAC diagnosis)².

Histopathological assessment

The pathological diagnosis of PDC was re-evaluated with H&E sections according to the 2019 WHO classification of tumors of the digestive system and graded based on the UICC TNM classification of malignant tumors [T stage (T3-4/T1-2), N stage (N1-2/N0), TNM stage (III-IV/I-II)] (8th edition) by three pathologists (X.P., H.M., and K.K.) in a blinded manner¹⁹. The histological grade was divided into three categories of well (well), moderately (mod), and poorly differentiated

adenocarcinoma (por)¹⁹. The highest grade in the sections represented the histological grade of the individuals regardless of the proportion¹⁹. Venous invasion was assessed on tumor sections stained with Elastica-von Gieson. Lymphatic invasion was evaluated on immunostained sections for podoplanin. The degree of invasion to venules and lymph vessels was graded as 0 (none), 1 (0-3 sites), 2 (3-6 sites), and 3 (>6 sites) within 10 high-power fields.

Methylation-specific PCR

Methylation-specific PCR (MSP) was performed using methods described in a previous study^{1,20}. MSP primer sequences for *PMS2* were designed with Methprimer (www.urogene.org/methprimer2/) as follows: 5'-GGTCGGTTCGGTATAGATGTC-3' (MF) and 5'-ACGTACAAATAAAAACGCGAA-3' (MR) for methylated genes; 5'-TTTGGTTGGTTGGTATAGATGTT-3' (UF) and 5'-ACCACATACAAATAAAAACACAAA-3' (UR) for unmethylated genes. The amplification conditions involved in this reaction were as follows: 98°C for 5 min, (98°C for 10 s, 62°C for 30 s, and 72°C for 30 s) × 35, 20°C ∞ for methylation primers; 98°C for 5 min, (98°C for 10 s, 57°C for 30 s, and 72°C for 30 s) × 35, 20°C ∞ for unmethylation primers. If unmethylated and methylated bands were concurrently observed, we judged the subjects as 'methylated'.

Immunohistochemistry

Immunohistochemistry was performed with 4 μm thick sections of paraffin-embedded tissue specimen as described elsewhere^{1,20,21}. The slides were incubated at 4°C overnight with different primary antibodies shown in Table S1.

For evaluation of MMR proteins, 10 representative areas were selected at 100× magnification on each slide. Then, the total cells scoring positive, intermediate, and negative were counted at 200× magnification. Staining in stromal and inflammatory cells was used as an internal control as positive. No expression of *PMS2* was judged as negative, and an intermediate staining pattern between positive and negative was judged as negative. The number of positive cells was divided by the total number of cells to obtain the positive rate. The same method was used to calculate the average value of 10 areas. A five-tiered scoring system (scores 0-4) was used for the positive rate as follows: 0 (0-4%), 1 (5-25%), 2 (26-50%), 3 (51-75%), and 4 (76-100%)⁷. If one or several of the four MMR proteins scored 0 or 1-4, the tumor was IHC classified as MMR-deficient (dMMR) or MMR-proficient (pMMR), respectively. The subjects were further classified into the *PMS2*_{Low} group or *PMS2*_{High} group based on a *PMS2* score of 0-2 or 3-4.

Evaluation of 8'-hydroxy-2'-deoxyguanosine (8-OHdG) was performed using the German Immunoreactive Score²². A staining intensity score [0 (no staining), 1 (weak staining), 2 (moderate staining), and 3 (strong staining)] and a staining proportion score [0 (no staining), 1 (1-10%), 2 (11-50%), 3 (51-80%), and 4 (81-100%)] were given, which were multiplied to obtain the total score.

For evaluation of CD8⁺ T cells and CD163⁺ TAMs, 10 representative areas were selected at 100× magnification on each slide. Then, positive cells were counted at ×200 magnification. The average value was calculated after obtaining the total number of positive cells in 10 areas.

Cell culture

The breast adenocarcinoma cell line MCF-7 and 4 PDAC cell lines, MIA PaCa-2, PANC-1, Bxpc-3, and AsPC-1, were purchased from the American Type Culture Collection (Manassas, VA, USA) and were cultured in low-glucose or high-glucose (25 mM) Dulbecco's modified Eagle medium (DMEM) (Fuji-film Wako Pure Chemical Corp., Osaka, Japan) supplemented with 10% fetal bovine serum (FBS) (Biosera, French Origin) and 1% penicillin–streptomycin (Thermo Fischer Scientific Corp., Waltham, MA, USA). The cells were cultured at 37°C in a humidified atmosphere of 5% CO₂. Each experiment was repeated three times.

Palmitic acid preparation and ROS measurement

Palmitic acid (Sigma–Aldrich, St Louis, MO, USA) was dissolved in 0.01 mM NaOH at 90°C for 10 min. Then, the clear solution was complexed with 5% fatty acid-free bovine serum albumin (BSA; Sigma–Aldrich) and shaken gently at 37°C for 2 h. The complexed palmitic acid solution was added to the cell culture medium to obtain the indicated final palmitic acid concentration. *N*-Acetyl-L-cysteine (NAC; Sigma–Aldrich) dissolved in phosphate-buffered saline (PBS) was added to the culture medium, and the final concentration was 5 mM. To determine the ROS levels, the cells were stained with 10 μM 2',7'-dichlorofluorescein diacetate (Sigma–Aldrich) dissolved in PBS for 30 min in the dark at 37°C. The ROS generation from mitochondria was evaluated by a Mitochondrial ROS Detection Kit (Cayman Chemical, Ann Arbor, MI, USA). The fluorescence was measured with a FlexStation 3 (Molecular Devices, San Jose, CA, USA).

Western blot

Western blotting was performed as described previously.²¹ The primary antibodies used in this study were shown in Table S1.

Quantitative evaluation of the mRNA expression

Real-time PCR was performed with cDNA generated from total RNA extracted from cell lysates as described previously^{21,22}. Commercially available primer and probe sets were used (Gene Expression Assay, Thermo Fisher Scientific.)

Statistical analysis

The relationship between two variables was determined by Student's *t*-test or the Mann–Whitney *U* test. The Pearson χ^2 test or Fisher's exact test was performed to compare the qualitative variables. Survival curves were analyzed by the Kaplan–Meier method with the log-rank test. A Cox proportional hazard model was performed to identify independent risk factors. All

statistical analyses were conducted with SPSS statistical software (version 22.0; IBM SPSS) and GraphPad Prism software (version 8.0; GraphPad Software). All *P* values were two-tailed, and significant differences were considered when *P* < 0.05.

RESULTS

Clinical characteristics of the PDAC subjects

The prevalence of obesity in the short-DM group was significantly higher than that of the NDM and long-DM groups (*P* < 0.01, respectively), possibly indicating the less physical exhaustion in the short-DM group than in the NDM and long-DM group (Table 1). Relative to the NDM group, both the short-DM group (*P* < 0.001 for preoperative, *P* < 0.05 for postoperative) and the long-DM group (*P* < 0.01 for both) had poor preoperative and postoperative glycohemoglobin A1c (HbA1c). The preoperative HbA1c levels in the DM group were substantially improved after surgery (*P* < 0.05), which was especially evident in the short-DM group (*P* < 0.01), while the influences were minimal in the long-DM group. The short-DM group exhibited a smaller tumor size (*P* < 0.05), lower postoperative HbA1c level (*P* < 0.05), and a higher Δ HbA1c (*P* < 0.01) than the long-DM group. Furthermore, patients with both short- and long-DM were likely to have concurrent dyslipidemia. A higher level of CEA was associated with DM (*P* < 0.05), particularly in the long-DM group. The effects of diabetes therapy were comparable among the diabetic groups.

PMS2 expression was downregulated in PDAC subjects complicated with DA

The expression of MSH6 was upregulated (*P* < 0.05 vs NDM), while degradation of PMS2 occurred in the DM group (*P* < 0.01) (Figure 1a, b). Although there were five cases with an absence of PMS2 expression in the DM group (*P* < 0.05), DA did not influence the MMR status, when the traditional definition of dMMR was applied (Figure 1c). Moreover, PMS2 scores in the short-DM group and long-DM group were significantly lower than those in the NDM group (*P* < 0.01, Figure 1d). Overall, considering that there were only a small number of cases with a complete absence of PMS2, the cases were stratified into a PMS2_{Low} group or PMS2_{High} group according to a PMS2 score of 0–2 or 3–4 based on the IHC results. The relationships between PMS2 expression and the clinicopathological parameters are summarized in Table 2. The PMS2_{Low} group was associated with poor differentiation (*P* < 0.05), advanced T stage (*P* < 0.05), diabetes (*P* < 0.001), higher HbA1c (*P* < 0.001), and dyslipidemia (*P* < 0.05).

Promoter methylation of *PMS2* was analyzed in PDAC tissues by MSP (Figure 1e). The frequency of hypermethylation of *PMS2* was similar in the DM and NDM groups (17.2% vs 15.6%, Figure 1f). On account of the relationship between dyslipidemia, DM, and *PMS2*, the patients were divided into two groups according to the presence of dyslipidemia. The *PMS2* score in the dyslipidemia group (DLP) was lower than that in the nondyslipidemia (NDLP) group (*P* < 0.05, Figure 1g).

Table 1 | Correlation between clinicopathological parameters and diabetic status

Parameter	NDM (n = 32)	Short-DM (n = 14)	Long-DM (n = 15)	DM (n = 29)
Gender, male, n (%)	11 (34.4%)	8 (57.1%)	7 (46.7%)	15 (51.7%)
Age (years)	68.7 ± 6.2	65.1 ± 7.9	67.2 ± 8.5	66.2 ± 8.1
BMI (kg/m ²)	22.2 ± 3.9	23.4 ± 3.2	22.1 ± 3.2	22.7 ± 3.2
History of obesity (BMI ≥ 25)	7 (21.9%)	6 (42.9%)*	3 (20.0%) [†]	9 (31.0%)
Tumor site, head, n (%)	21 (65.6%)	9 (64.3%)	10 (66.7%)	19 (65.5%)
Histological grade, poor, n (%)	10 (31.3%)	8 (57.1%)	8 (53.3%)	16 (55.2%)
Tumor size (mm)	38.1 ± 19.3	32.2 ± 8.5	41.3 ± 13.7 [‡]	36.9 ± 12.2
T stage, T3–4, n (%)	19 (59.4%)	8 (57.1%)	11 (73.3%)	19 (65.5%)
N stage, N1–2, n (%)	21 (65.6%)	10 (71.4%)	13 (86.7%)	23 (79.3%)
TNM stage, III–IV, n (%)	20 (62.5%)	8 (57.1%)	9 (60.0%)	17 (58.6%)
HbA1c (NGSP, %):				
Pre-operation	5.7 ± 0.6	8.1 ± 1.9 [§]	7.6 ± 1.9 [§]	7.9 ± 1.9 [§]
Post-operation	5.9 ± 0.8	6.9 ± 1.3 ^{¶¶}	7.6 ± 1.7 ^{‡§}	7.3 ± 1.5 [§] **
ΔHbA1c (%) [(pre-post) operation]	−0.3 ± 0.6	1.2 ± 0.8 [§]	0.2 ± 0.8 ^{††}	0.6 ± 1.0 [§]
Diabetes therapy				
OHA, n (%)	0 (0.0%)	10 (71.4%)	12 (80.0%)	22 (75.9%)
Insulin, n (%)	0 (0.0%)	3 (21.4%)	5 (33.3%)	8 (27.6%)
Dyslipidemia, n (%)	11 (34.4%)	11 (78.6%) [¶]	10 (66.7%) [¶]	21 (72.4%) [¶]
CEA (ng/mL)	3.1 ± 1.9	4.0 ± 1.8	7.0 ± 9.5 [¶]	5.5 ± 7.0 [¶]

* $P < 0.01$ vs NDM, [†] $P < 0.01$ vs short-DM, [‡] $P < 0.05$ vs short-DM group, [§] $P < 0.001$ vs NDM group, [¶] $P < 0.05$ vs NDM group, ^{¶¶} $P < 0.001$ vs HbA1c (%) (pre-operation), ^{**} $P < 0.05$ vs HbA1c (%) (pre-operation), ^{††} $P < 0.001$ vs short-DM group. BMI, body mass index; CEA, carcinoembryonic antigen; DM, diabetes mellitus; HbA1c, glycohemoglobin A1C; NDM, non-diabetes mellitus; NGSP, National Glycohemoglobin Standardization Program; OHA, oral hypoglycemic agent; poor, poor differentiation.

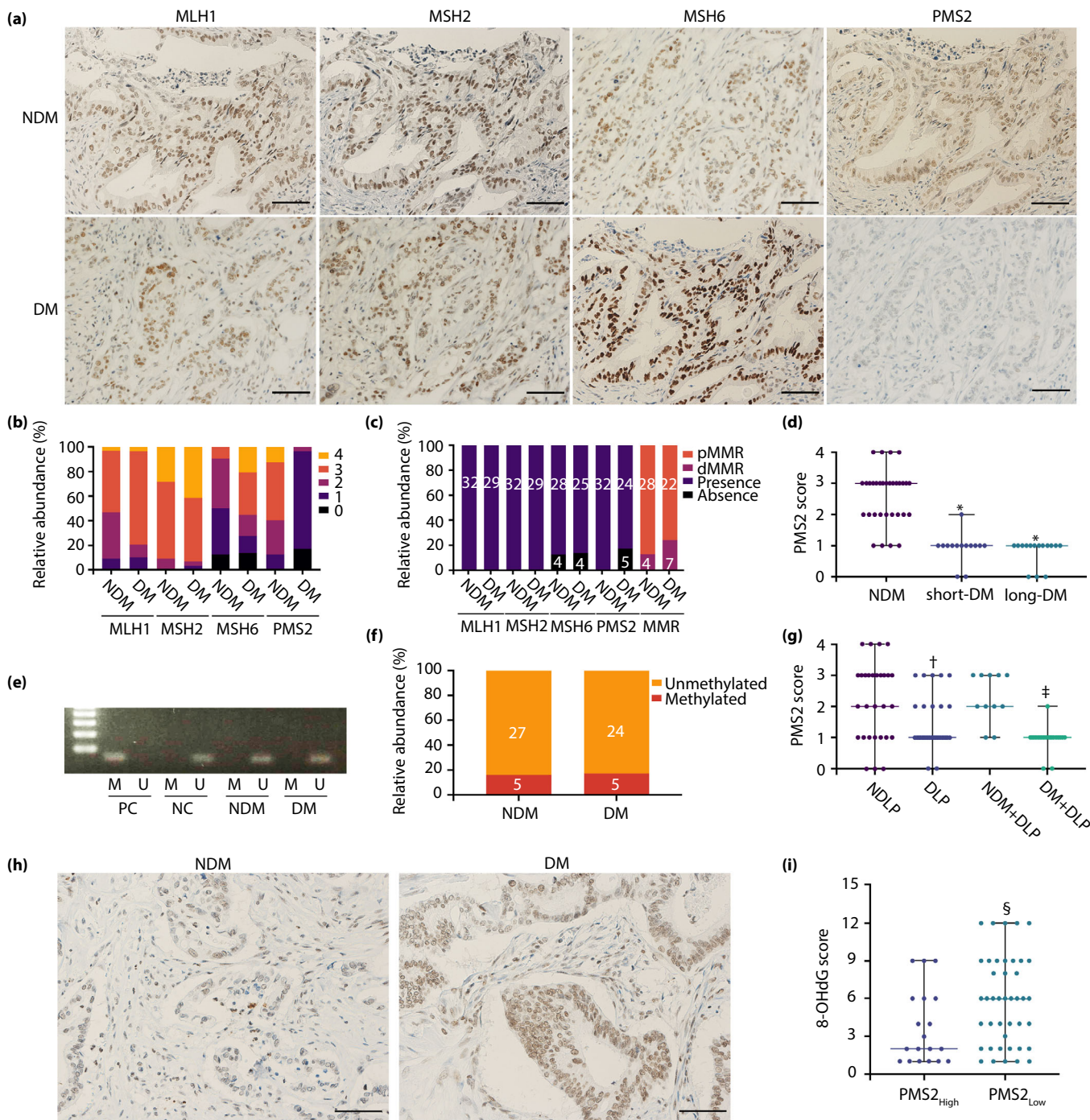
Dyslipidemia was strongly correlated with DM ($P < 0.001$, Figure 1g). To assess the involvement of oxidative stress, immunostaining for 8-OHdG was performed (Figure 1h). In the NDM subjects, a faint positive reaction for 8-OHdG was observed in the nucleus of PDAC cells. Conversely, 8-OHdG was more frequently and robustly expressed in the nucleus of PDAC cells from patients with DA. The PMS2_{Low} group had a higher 8-OHdG score than the PMS2_{High} group ($P < 0.05$, Figure 1i).

Palmitic acid with high glucose induced downregulation of PMS2 protein through the ROS pathway *in vitro*

MMR proteins were found to be stably expressed in various kinds of PDAC cell lines, similar to the breast cell line MCF-7,

which is proficient in MMR (Figure S1). MIAPaCa-2 and PANC-1 were chosen because of their robust expression of PMS2. The expression of PMS2 protein was comparable in the high-glucose (25 mM) group and the low-glucose (5.5 mM) group (Figure 2a, b). Because the frequency of dyslipidemia was high in the PMS2_{Low} group, these tumor cells were challenged with different concentrations of palmitic acid for 24 h. In the low-glucose group, a high dose of palmitic acid (500 μM) slightly induced the degradation of PMS2 in MIAPaCa-2 ($P < 0.05$) and PANC-1 ($P < 0.05$) cells after 24 h (Figure 2a, b). Notably, the effect of a low dose of palmitic acid (100 μM) was strengthened when combined with high glucose ($P < 0.05$). Meanwhile, there were no substantial changes in the other MMR proteins, especially MLH1. The mRNA level of

Figure 1 | PMS2 expression was downregulated in PDAC subjects complicated with DA. (a) MMR protein expression evaluated in immunochemistry. (b) The expression of MMR is semiquantitatively scored from 0 to 4 in the non-DA (NDM) group and DM group. (c) Comparison of MMR status in the NDM group and DM group. (d) Comparison of PMS2 scores in the NDM group, short-DM group, and long-DM group. (e–f) Promoter methylation of *PMS2* is evaluated in the NDM group and DM group (e). Completely CpG-methylated HeLa genomic DNA is used as a positive control (PC). Completely CpG unmethylated HCT116 DKO genomic DNA is used as a negative control (NC). The prevalence of promoter methylation of *PMS2* is shown in f. (g) Comparison of PMS2 scores in the NDLP group, DLP group, NDM + DLP group, and DM + DLP group. (h) The NDM group shows high expression of PMS2 with low expression of 8-OHdG. The DM group shows low PMS2 expression with high 8-OHdG expression. (i) Comparison of 8-OHdG scores in the PMS2_{High} group and PMS2_{Low} group. DA, diabetes mellitus; DLP, dyslipidemia; dMMR, MMR-deficient; MLH1, MutL homolog 1; MMR, mismatch repair; MSH2, MutS homolog 2; MSH6, MutS homolog 6; NDLP, nondyslipidemia; PDAC, pancreatic ductal adenocarcinoma; PMS2, PMS1 Homolog 2; pMMR, MMR-proficient; 8-OHdG, 8-hydroxy-2'-deoxyguanosine. The data are presented as the mean ± SD. P values < 0.05 were considered significant; * $P < 0.01$ vs NDM, [†] $P < 0.05$ vs NDLP; [‡] $P < 0.01$ vs NDM + DLP, [§] $P < 0.05$ vs PMS2_{High} group. The bar is 100 μm (a, h).



PMS2 was significantly downregulated similar to the protein level of PMS2 in response to palmitic acid and glucose stimulation in both cell lines (Figure 2c, d).

Palmitic acid (100 μ M) with high glucose (PA + HG) was selected to stimulate PDAC cells with or without an antioxidant 5 mM NAC. Although the ROS generation from mitochondria induced by PA + HG was unchanged, the elevated total level of ROS induced by PA + HG could be suppressed by NAC in

tumor cells (Figure 2e, f). Western blot analysis also revealed that the downregulation of PMS2 protein caused by PA + HG could be restored by NAC (Figure 2g, h).

Presence of DA-modified immune cell infiltration in PDAC

Representative images of the density of CD8⁺ T cells and CD163⁺ TAMs are shown in Figure 3a. The presence of DA and a long duration of DA had no impact on the infiltration of

Table 2 | Correlation between clinicopathological parameters and PMS2

Parameter	PMS2 _{Low} (n = 42)	PMS2 _{High} (n = 19)
Gender, male	19 (45.2%)	7 (36.8%)
Age ≥ 65 years old	30 (71.4%)	12 (63.2%)
BMI ≥ 25 kg/m ²	9 (21.4%)	7 (36.8%)
Tumor site, head	28 (66.6%)	12 (63.2%)
Histological grade, por	22 (52.4%)	4 (21.1%)*
Tumor size >4 cm	10 (23.8%)	7 (36.8%)
T stage, T3–4	30 (71.4%)	8 (42.1%)*
N stage, N1–2	31 (73.8%)	13 (68.4%)
TNM stage, III–IV	28 (66.6%)	9 (47.4%)
HbA1c ≥ 7.0% (pre-operation)	22 (52.4%)	0 (0.0%) [†]
DM	29 (69.0%)	0 (0.0%) [†]
Long-DM	15 (35.7%)	0 (0.0%) [†]
Short-DM	14 (33.3%)	0 (0.0%) [†]
Dyslipidemia	27 (64.3%)	5 (26.3%)*
CEA >5.68 ng/mL	8 (19.0%)	3 (15.8%)

* $P < 0.05$ vs PMS2_{low}, [†] $P < 0.001$ vs PMS2_{low}. BMI, body mass index; CEA, carcinoembryonic antigen; DM, diabetes mellitus; HbA1c, glycohemoglobin A1C; por, poor differentiation.

CD8⁺ T cells in PDAC (Figure 3b). In contrast, the short-DM group showed a significant increase in CD8⁺ T-cell infiltration compared with the NDM group ($P < 0.05$). As expected, the PMS2_{Low} group had a higher density of CD8⁺ T cells than the PMS2_{High} group ($P < 0.05$, Figure 3c). However, the number of CD163⁺ TAMs in the DM group was significantly higher than that in the NDM group ($P < 0.05$, Figure 3d). In contrast to the CD8⁺ T cells, the infiltration of CD163⁺ TAMs was significantly increased in the long-DM group compared with the short-DM group and the NDM group ($P < 0.05$, respectively) but not in the short-DM group compared with the NDM group.

Different durations of DA influenced PDAC prognosis via changes of PMS2 expression and immune cells

Kaplan–Meier curves with a log-rank test showed that overall survival (OS) and disease-free survival (DFS) were comparable between the non-DM group and the DM group, while the short-DM patients had longer overall survival and disease-free

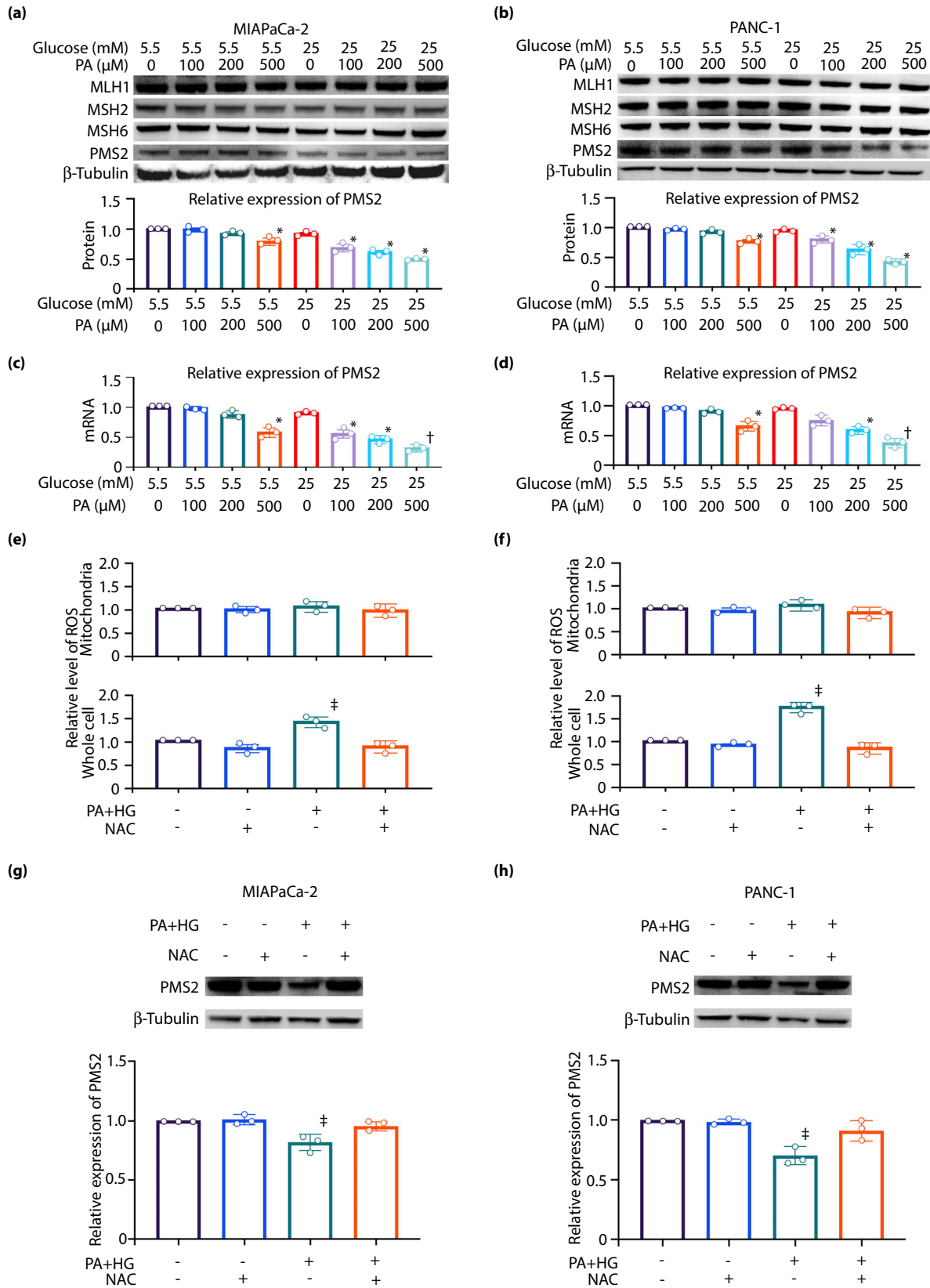
survival than the NDM patients ($P < 0.05$, respectively) (Figure 4a, b). The long-DM patients had shorter overall survival and disease-free survival than the NDM patients ($P < 0.05$, respectively). A low expression of PMS2 may contribute to a better prognosis of short DM because they were apparently associated with better overall survival ($P < 0.05$ for PMS2, Figure 4c) and disease-free survival ($P < 0.05$ for PMS2, Figure 4d). The effects of a low expression of PMS2 on disease-free survival and overall survival disappeared in the subjects of long-term diabetes (Figure 4e, f).

The Cox proportional hazard model showed that in univariate analysis, tumor size > 4 cm ($P < 0.05$), long-DM ($P < 0.01$), and low expression of PMS2 ($P < 0.01$) were considered prognostic factors for DFS, and CEA >5.68 ng/mL ($P < 0.05$), long-DM ($P < 0.01$), and low expression of PMS2 ($P < 0.01$) were confirmed as factors for OS (Table 3). Multivariate analysis further confirmed that long-DM (HR = 4.928, 95% CI = 2.102–11.552, $P < 0.001$) and low expression of PMS2 (HR = 0.288, 95% CI = 0.134–0.621, $P = 0.001$) were statistically independent factors for DFS. Long-DM (HR = 6.931, 95% CI = 2.772–17.334, $P < 0.001$) and low expression of PMS2 (HR = 0.186, 95% CI = 0.073–0.474, $P < 0.001$) were also identified as independent predictors of OS in PDAC.

DISCUSSION

The isolated loss of PMS2 expression by immunohistochemistry is a rare finding in various types of carcinoma^{23,24}. The most common molecular alteration found in such cases is a germline mutation in the *PMS2* and *MLH1* genes²³, but our results showed that DA could downregulate the protein expression of PMS2 and increase MSH6 in PDAC. Diabetes could increase the frequency of promoter hypermethylation of *CDH1* in PDAC and *DPYSL3* in hepatocellular carcinoma^{1,20}, while, no evidence was found for diabetes causing promoter hypermethylation of *PMS2*. Intriguingly, the protein and mRNA expression levels of PMS2 are downregulated as the oxidative stress increases during the progression of several types of tumors^{25,26}. Generally, oxidative stress has been found to play an essential role in diabetes and the pathogenesis of diabetic complications^{22,27,28}. However, in streptozotocin-induced diabetic rat kidneys, PMS2 expression was suppressed only in the

Figure 2 | Palmitic acid with high glucose induced the downregulation of PMS2 protein through the ROS pathway *in vitro*. (a, b) Expression of MMR proteins in MIAPaCa-2 (a) and PANC-1 (b) cells cultured in low-glucose (5.5 mM) or high-glucose (25 mM) medium by western blot analysis, after stimulation with different concentrations of palmitic acid for 24 h. BSA alone is added as a control. (c, d) mRNA expression of PMS2 in MIAPaCa-2 (a) and PANC-1 (b) cells cultured in the same condition as a and b. (e, f) In the presence or absence of 5 mM NAC, ROS levels from mitochondria and whole cells are detected in MIAPaCa-2 (e) and PANC-1 (f) cells cultured with or without 100 μM PA + high glucose (PA + HG). BSA alone is added as a control. (g, h) Western blot analysis shows PMS2 expression in MIAPaCa-2 cells (g) and PANC-1 cells (h) cultured with or without PA + HG in the presence or absence of 5 mM NAC. BSA alone is added as a control. BSA, bovine serum albumin; HG, high glucose; MLH1, MutL homolog 1; MMR, mismatch repair; MSH2, MutS homolog 2; MSH6, MutS homolog 6; NAC, N-acetyl-L-cysteine; PA, palmitic acid; PMS2, PMS1 homolog 2; ROS, reactive oxygen species. The data are presented as the mean ± SD. P values <0.05 are considered significant. * $P < 0.05$ vs 5.5 mM glucose without PA, [†] $P < 0.01$ vs 5.5 mM glucose without PA, [‡] $P < 0.05$ vs 5.5 mM glucose without PA + HG and NAC.



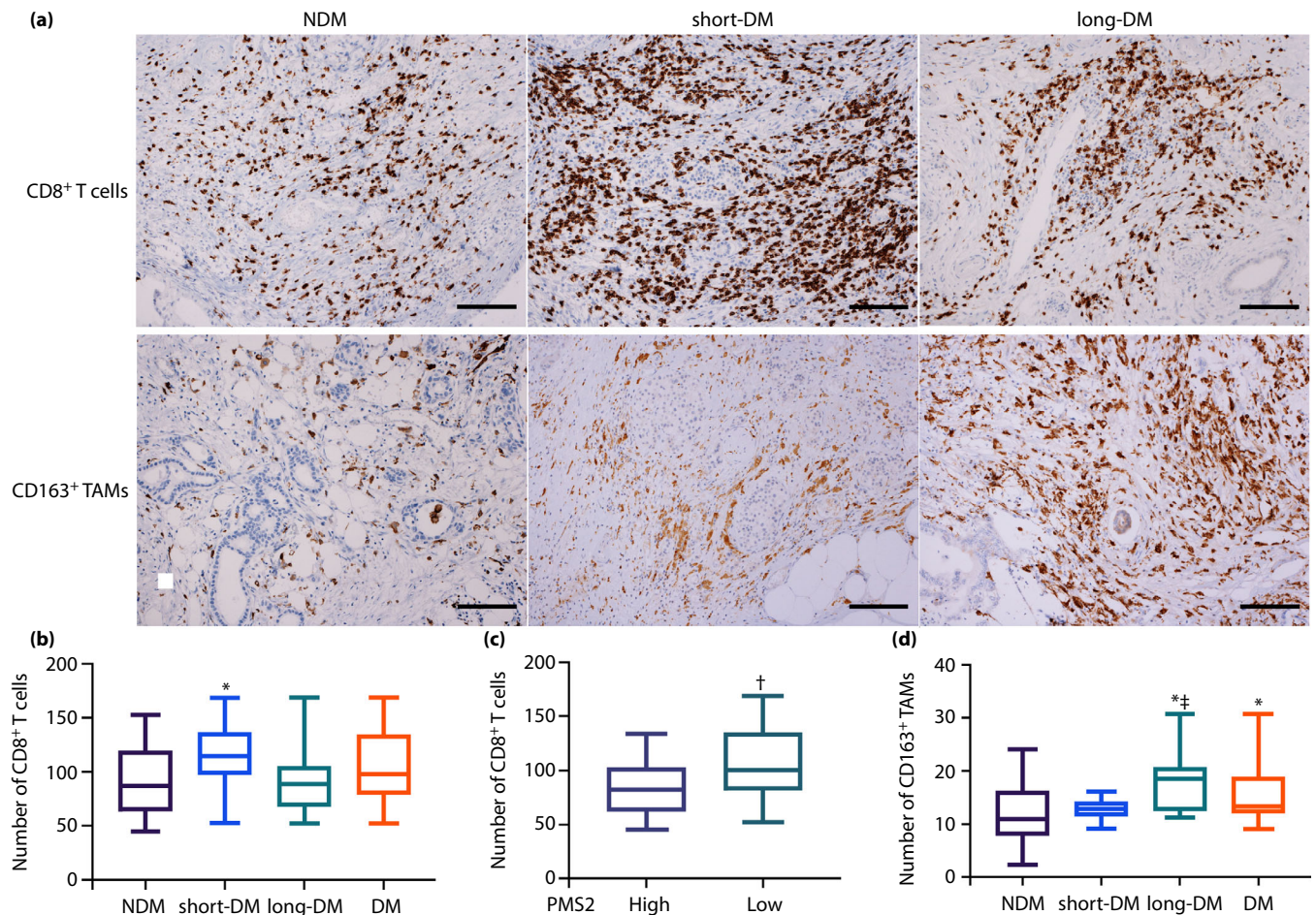
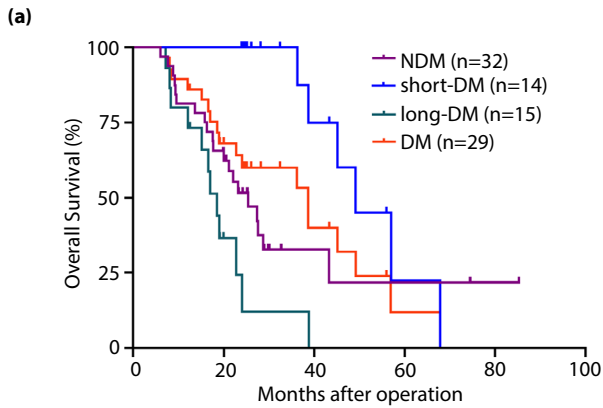


Figure 3 | DA modified immune cell infiltration in PDAC. (a) Representative images show the density of CD8⁺ T cells and CD163⁺ TAMs in the NDM group, short-DM group, and long-DM group. (b) Comparison of the number of CD8⁺ T cells in the NDM group, short-DM group, long-DM group, and DM group. (c) Comparison of the number of CD8⁺ T cells in the PMS2_{High} group and PMS2_{Low} group. (d) Comparison of the number of CD163⁺ TAMs in the NDM group, short-DM group, long-DM group, and DM group. CD8, cluster of differentiation 8; CD163, cluster of differentiation 163; DA, diabetes mellitus; PDAC, pancreatic ductal adenocarcinoma; TAMs, tumor-associated macrophages. The data are presented as the mean \pm SD. *P* values <0.05 are considered significant. **P* < 0.05 vs NDM, [†]*P* < 0.05 vs PMS2 High, [‡]*P* < 0.05 vs short-DM. The bar is 200 μ m.

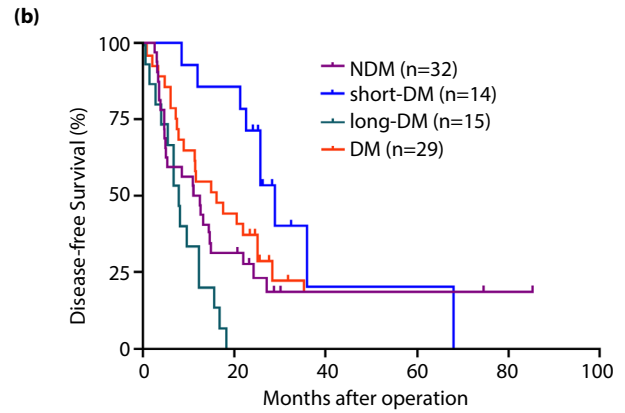
glomeruli, but not in the tubules²⁹. This might indicate that PMS2 expression can be changed in a tissue specific manner, possibly due to the differences in oxidative stress sensitivity. This suggests that MMR proteins may be differentially degraded by diabetes in different kinds of carcinoma. Thus, it would be necessary to evaluate the change of PMS2 expression elicited by diabetes in other types of cancer than PDAC in the future.

Our results showed that the ROS production was elicited by high glucose and high palmitic acid as reported previously^{21,30}, while they did not largely depend on the mitochondria of PDAC cells. ROS can be generated by glucose in several pathways other than oxidative phosphorylation in the mitochondria of cancer cells: glyceraldehyde autoxidation, PKC activation, glycation, sorbitol metabolism, and hexosamine pathway³¹. Meanwhile, palmitic acid can also increase ROS production

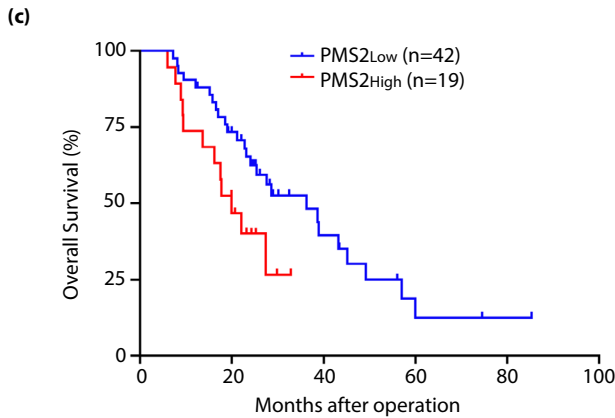
Figure 4 | Different durations of DA influenced PDAC prognosis *via* PMS2 and immune cells. (a, b) Kaplan–Meier analysis of overall survival (OS, a) and disease-free survival (DFS, b) between the NDM group, short-DM group, long-DM group, and DM group. (c, d) Kaplan–Meier analysis of OS (c) and DFS (d) between the high and low expression of PMS2 groups. (e, f) Kaplan–Meier analysis of OS (e) and DFS (f) between the NDM group, short-DM group, and long-DM group showing low expression of PMS2. DA, diabetes mellitus; PDAC, pancreatic ductal adenocarcinoma; PMS2, PMS1 homolog 2. *P* values <0.05 are considered significant.



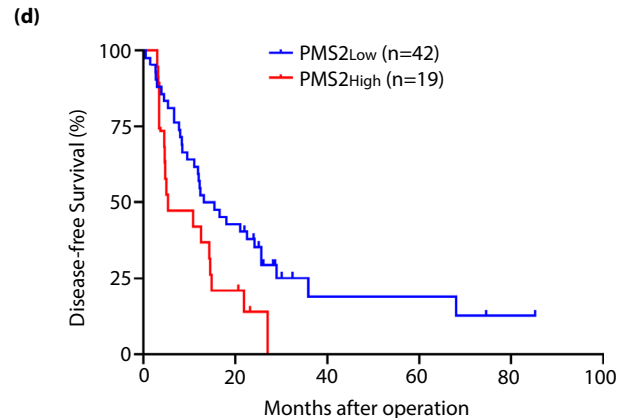
	Meidan OS (months)	P value
NDM vs. DM	25.4 vs. 38.7	0.524
NDM vs. short-DM	25.4 vs. 49.2	< 0.05
NDM vs. long-DM	25.4 vs. 18.6	< 0.05
short-DM vs. long-DM	49.2 vs. 18.6	< 0.001



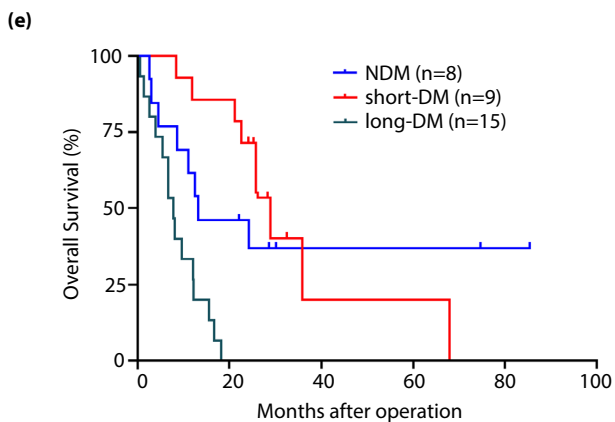
	Meidan DFS (months)	P value
NDM vs. DM	11.8 vs. 15.5	0.647
NDM vs. short-DM	11.8 vs. 28.9	< 0.05
NDM vs. long-DM	11.8 vs. 7.8	< 0.05
short-DM vs. long-DM	28.9 vs. 7.8	< 0.001



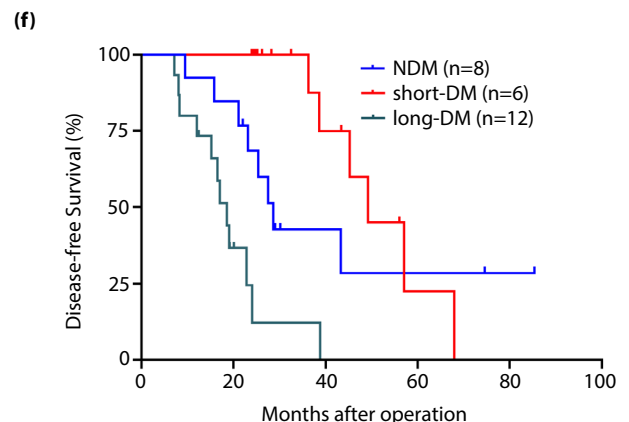
	Meidan OS (months)	P value
PMS2Low vs. PMS2High	36.3 vs. 20.1	< 0.05



	Meidan DFS (months)	P value
PMS2Low vs. PMS2High	14.4 vs. 5.4	< 0.05



	Meidan OS (months)	P value
NDM vs. short-DM	28.7 vs. 49.2	0.201
NDM vs. long-DM	28.7 vs. 18.6	< 0.01
short-DM vs. long-DM	49.3 vs. 18.6	< 0.001



	Meidan DFS (months)	P value
NDM vs. short-DM	13.2 vs. 28.9	0.636
NDM vs. long-DM	13.2 vs. 7.8	< 0.01
short-DM vs. long-DM	28.9 vs. 7.8	< 0.001

Table 3 | Cox proportional hazard model of PDAC

Parameter (n = 61)	Disease-free survival						Overall survival					
	Univariate			Multivariate			Univariate			Multivariate		
	HR	95%CI	P value	HR	95%CI	P value	HR	95% CI	P value	HR	95% CI	P value
Gender, male	0.820	0.463–1.451	0.495	–	–	–	0.662	0.342–1.283	0.222	–	–	–
Age ≥ 65 years old	1.373	0.736–2.560	0.319	–	–	–	1.067	0.537–2.119	0.853	–	–	–
BMI ≥ 25 kg/m ²	0.565	0.280–1.140	0.111	–	–	–	0.660	0.273–1.596	0.356	–	–	–
Histological grade, por	0.698	0.391–1.245	0.223	–	–	–	0.883	0.463–1.684	0.706	–	–	–
Tumor size > 4 cm	2.241	1.209–4.151	0.010	1.322	0.687–2.542	0.403	1.564	0.761–3.215	0.224	–	–	–
T stage, T3–4	1.092	0.604–1.975	0.77	–	–	–	0.755	0.388–1.472	0.410	–	–	–
N stage, N1–2	1.606	0.831–3.104	0.158	–	–	–	1.817	0.824–4.007	0.139	–	–	–
TNM stage, III–IV	1.014	0.564–1.824	0.962	–	–	–	0.585	0.303–1.129	0.110	–	–	–
HbA1c ≥ 7.0% (pre-operation)	0.865	0.478–1.565	0.631	–	–	–	0.843	0.428–1.662	0.622	–	–	–
Diabetes therapy: OHA	0.972	0.548–1.722	0.922	–	–	–	0.821	0.421–1.604	0.564	–	–	–
Diabetes therapy: insulin	1.775	0.783–4.025	0.170	–	–	–	1.357	0.562–3.273	0.497	–	–	–
Dyslipidemia	0.924	0.525–1.627	0.785	–	–	–	1.164	0.612–2.214	0.644	–	–	–
CEA > 5.68 ng/mL	1.038	0.501–2.151	0.919	–	–	–	2.485	1.141–5.410	0.022	2.898	1.303–6.444	0.009
Long-duration DM	2.952	1.528–5.701	0.001	4.928	2.102–11.552	< 0.001	3.381	1.616–7.073	0.001	6.931	2.772–17.334	< 0.001
PMS2, low	0.877	0.500–1.540	0.648	–	–	–	0.811	0.424–1.548	0.525	–	–	–
	0.504	0.273–0.928	0.028	0.288	0.134–0.621	0.001	0.468	0.223–0.982	0.045	0.186	0.073–0.474	< 0.001

BMI, body mass index; CEA, carcinoembryonic antigen; CI, confidence interval; DM, diabetes mellitus; HbA1c, glycohemoglobin A1C; HR, hazard ratio; OHA, oral hypoglycemic agent; por, poor differentiation.

without mitochondria in PDAC cells³². Thus, our results confirm that mitochondria would not play a pivotal role in the generation of ROS in response to high glucose and palmitic acid in PDAC cells.

A previous study revealed that dMMR is associated with a high density of CD8⁺ T cells, which is assumed to be related to a better prognosis¹⁷. Lynch syndrome caused by PMS2 mutations also exhibits a better prognosis^{23,33,34}. Similarly, short-term DM showed a better overall survival and disease-free survival than NDM in this study. The infiltration of CD8⁺ T cells in PDAC tissues was not influenced by the diabetic status, consistent with previous studies in peripheral blood³⁵. However, a high density of CD8⁺ T cells was found in the short-DM group compared with the NDM and long-DM groups. These findings may imply that the DNA mismatch repair ability is attenuated and MSI is high in short-DM, even if PMS2 is not lost completely. Because immune checkpoint inhibitors are effective in MSI-H carcinoma with CD8⁺ T-cell infiltration, our results suggest that an immune checkpoint inhibitor can be a beneficial therapeutic option for PDAC with a short duration of DA.

Through the education of tumors, macrophages that participate in the constitution of the TME will be transformed into immunosuppressed M2-like TAMs (CD163⁺) in large numbers to support tumor growth and metastasis, leading to a poor prognosis^{36,37}. A previous study validated that hyperglycemia enhanced the polarization of macrophages with protumor properties *in vitro* and reduced the production of TNF- α ^{38–40}. Meanwhile, peritoneal macrophages with the M2-like type were activated in animals with a long duration of diabetes *via* the ERK and AKT pathways^{41,42}. In a similar perspective, we demonstrated that M2-like TAMs were more strongly associated with long-DM than with short-DM. In several types of cancer models, TAMs have been proven to impair the antitumor roles of CD8⁺ T cells^{43–45}. Therefore, we hypothesized that a high density of CD163⁺ TAMs induced by long-DM could suppress CD8⁺ T cells associated with low expression of PMS2, resulting in a worse prognosis of PDAC with long-DM. In addition, long-DM is associated with a high frequency of *CDH1* promoter methylation and activation of pancreatic stellate cells, leading to tumor cell metastasis *via* epithelial mesenchymal transition^{1,21}. Thus, factors other than TAMs can synergistically contribute to tumor progression in long-DM. Although a high level of postoperative HbA1c may be ascribed to a worse prognosis, additional studies are required to explore the factors that worsen the prognosis of long-DM.

Decreased insulin secretion and insulin resistance are two important characteristics of DA, leading to hyperglycemia and increased free fatty acids (FFAs)¹³. Our results indicate that palmitic acid plus high glucose could reversibly reduce the expression of PMS2 protein through ROS generation *in vitro*. From a clinical point of view, the treatment intensity for such metabolic disturbances that maximizes the effects of downregulation of PMS2 in PDAC cells should be determined in the future.

There are several limitations of this research. First, the MSI status was not evaluated in this study, although we evaluated MSI status indirectly with immunohistochemistry for MMR proteins. To confirm our results, evaluation of the MSI status with the Bethesda panel of the Promega panel would be required in the future⁴⁶. Second, the prevalence of PDAC and precise changes in glycemic control were not directly evaluated because of the retrospective nature of the data. Future prospective studies will be necessary to confirm our data. Third, to clarify the detailed mechanism of how ROS downregulates PMS2 expression, upstream factors regulating PMS2 expression should be considered. Other pathways by which DA affects PMS2 also need to be explored urgently. Finally, CD163 is only one of the specific markers of M2-like TAMs and cannot completely cover all M2-polarized TAMs. More markers and promising multiplex immunohistochemistry/immunofluorescence are required to substitute for conventional immunohistochemistry to better label all subtypes of TAMs⁴⁷.

Taken together, our results suggest that the different phases of DA have a major impact on PDAC by affecting the expression of PMS2, which alters the tumor immune microenvironment. Proper glycemic control may change the TME, preventing the downregulation of PMS2 in PDAC. In particular, a short duration of diabetes may be a good indicator for an immune checkpoint inhibitor.

ACKNOWLEDGMENTS

The technical assistance of Misato Sakamoto, Hiroko Mori, Saeko Osanai, Saori Ogasawara, and Rumiko Imai is greatly appreciated.

DISCLOSURE

The authors declare no conflict of interest.

Approval of the research protocol: The use of paraffin blocks and study design were approved by the Ethics Committee of Hirosaki University School of Medicine (date of approval: 31 March 2022, approval number #2021–171), and the study protocol conforms to the provisions of the Declaration of Helsinki. Informed consent: N/A.

Registry and the registration no. of the study/trial: N/A.

Animal studies: N/A.

REFERENCES

- Saito T, Mizukami H, Umetsu S, *et al.* Worsened outcome in patients with pancreatic ductal carcinoma on long-term diabetes: association with e-cadherin1 (*cdh1*) promoter methylation. *Sci Rep* 2017; 7: 18056.
- Yuan C, Rubinson DA, Qian ZR, *et al.* Survival among patients with pancreatic cancer and long-standing or recent-onset diabetes mellitus. *J Clin Oncol* 2015; 33: 29–35.
- Hwang A, Narayan V, Yang YX. Type 2 diabetes mellitus and survival in pancreatic adenocarcinoma: a retrospective cohort study. *Cancer* 2013; 119: 404–410.

4. Jiricny J. The multifaceted mismatch-repair system. *Nat Rev Mol Cell Biol* 2006; 7: 335–346.
5. Humphris JL, Patch AM, Nones K, *et al.* Hypermutation in pancreatic cancer. *Gastroenterology* 2017; 152: e2.
6. Grant RC, Denroche R, Jang GH, *et al.* Clinical and genomic characterisation of mismatch repair deficient pancreatic adenocarcinoma. *Gut* 2021; 70: 1894–1903.
7. Ahmad-Nielsen SA, Bruun Nielsen MF, Mortensen MB, *et al.* Frequency of mismatch repair deficiency in pancreatic ductal adenocarcinoma. *Pathol Res Pract* 2020; 216: 152985.
8. Sugano K, Nakajima T, Sekine S, *et al.* Germline pms2 mutation screened by mismatch repair protein immunohistochemistry of colorectal cancer in Japan. *Cancer Sci* 2016; 107: 1677–1686.
9. Kasela M, Nystrom M, Kansikas M. PMS2 expression decrease causes severe problems in mismatch repair. *Hum Mutat* 2019; 40: 904–907.
10. Kansikas M, Kasela M, Kantelinen J, *et al.* Assessing how reduced expression levels of the mismatch repair genes mlh1, msh2, and msh6 affect repair efficiency. *Hum Mutat* 2014; 35: 1123–1127.
11. Nyström-Lahti M, Perrera C, Räschle M, *et al.* Functional analysis of mlh1 mutations linked to hereditary nonpolyposis colon cancer. *Genes Chromosomes Cancer* 2002; 33: 160–167.
12. Raevaara TE, Vaccaro C, Abdel-Rahman WM, *et al.* Pathogenicity of the hereditary colorectal cancer mutation hmlh1 del616 linked to shortage of the functional protein. *Gastroenterology* 2003; 125: 501–509.
13. Stumvoll M, Goldstein BJ, van Haefen TW. Type 2 diabetes: principles of pathogenesis and therapy. *Lancet* 2005; 365: 1333–1346.
14. Chang CL, Marra G, Chauhan DP, *et al.* Oxidative stress inactivates the human DNA mismatch repair system. *Am J Physiol Cell Physiol* 2002; 283: C148–C154.
15. Kato T, Noma K, Ohara T, *et al.* Cancer-associated fibroblasts affect intratumoral cd8(+) and foxp3(+) t cells via il6 in the tumor microenvironment. *Clin Cancer Res* 2018; 24: 4820–4833.
16. Farhood B, Najafi M, Mortezaee K. Cd8(+) cytotoxic t lymphocytes in cancer immunotherapy: a review. *J Cell Physiol* 2019; 234: 8509–8521.
17. Fraune C, Burandt E, Simon R, *et al.* Mmr deficiency is homogeneous in pancreatic carcinoma and associated with high density of Cd8-positive lymphocytes. *Ann Surg Oncol* 2020; 27: 3997–4006.
18. Seino Y, Nanjo K, Tajima N, *et al.* Report of the committee on the classification and diagnostic criteria of diabetes mellitus. *J Diabetes Invest* 2010; 1: 212–228.
19. Amin MB, Edge SB, Greene FL, *et al.* *Ajcc cancer staging manual*, 8th edn. Berlin: Germany, Springer, 2017.
20. Umetsu S, Mizukami H, Saito T, *et al.* Diabetes, an independent poor prognostic factor of non-B non-C hepatocellular carcinoma, correlates with dihydropyrimidinase-like 3 promoter methylation. *Sci Rep* 2020; 10: 1156.
21. Uchida C, Mizukami H, Hara Y, *et al.* Diabetes in humans activates pancreatic stellate cells via RAGE in pancreatic ductal adenocarcinoma. *Int J Mol Sci* 2021; 22: 11716.
22. Takahashi K, Mizukami H, Osonoi S, *et al.* Inhibitory effects of xanthine oxidase inhibitor, topiroxostat, on development of neuropathy in db/db mice. *Neurobiol Dis* 2021; 155: 105392.
23. Dudley B, Brand RE, Thull D, *et al.* Germline mlh1 mutations are frequently identified in lynch syndrome patients with colorectal and endometrial carcinoma demonstrating isolated loss of pms2 immunohistochemical expression. *Am J Surg Pathol* 2015; 39: 1114–1120.
24. Gill S, Lindor NM, Burgart LJ, *et al.* Isolated loss of pms2 expression in colorectal cancers: frequency, patient age, and familial aggregation. *Clin Cancer Res* 2005; 11: 6466–6471.
25. Hironaka K, Factor VM, Calvisi DF, *et al.* Dysregulation of DNA repair pathways in a transforming growth factor alpha/c-myc transgenic mouse model of accelerated hepatocarcinogenesis. *Lab Invest* 2003; 83: 643–654.
26. Javid M, Sasanakietkul T, Nicolson NG, *et al.* DNA mismatch repair deficiency promotes genomic instability in a subset of papillary thyroid cancers. *World J Surg* 2018 Feb; 42: 358–366.
27. Zhang P, Li T, Wu X, *et al.* Oxidative stress and diabetes: antioxidative strategies. *Front Med* 2020; 14: 583–600.
28. Inokuchi S, Itoh S, Yoshizumi T, *et al.* Mitochondrial expression of the DNA repair enzyme ogg1 improves the prognosis of pancreatic ductal adenocarcinoma. *Pancreatol* 2020; 20: 1175–1182.
29. Dragun M, Filipović N, Racetin A, *et al.* Immunohistochemical expression pattern of mismatch repair genes in the short-term streptozotocin-induced diabetic rat kidneys. *Appl Immunohistochem Mol Morphol* 2021; 29: e83–e91.
30. Li W, Ma Q, Li J, *et al.* Hyperglycemia enhances the invasive and migratory activity of pancreatic cancer cells via hydrogen peroxide. *Oncol Rep* 2011; 25: 1279–1287.
31. Robertson R, Zhou H, Zhang T, *et al.* Chronic oxidative stress as a mechanism for glucose toxicity of the beta cell in type 2 diabetes. *Cell Biochem Biophys* 2007; 48: 139–146.
32. Binker-Cosen MJ, Richards D, Oliver B, *et al.* Palmitic acid increases invasiveness of pancreatic cancer cells AsPC-1 through TLR4/ROS/NF- κ B/MMP-9 signaling pathway. *Biochem Biophys Res Commun* 2017; 484: 152–158.
33. ten Broeke SW, Brohet RM, Tops CM, *et al.* Lynch syndrome caused by germline pms2 mutations: delineating the cancer risk. *J Clin Oncol* 2015; 33: 319–325.
34. Senter L, Clendenning M, Sotamaa K, *et al.* The clinical phenotype of lynch syndrome due to germ-line pms2 mutations. *Gastroenterology* 2008; 135: 419–428.
35. Miya A, Nakamura A, Miyoshi H, *et al.* Impact of glucose loading on variations in CD4⁺ and CD8⁺ T cells in japanese

- participants with or without type 2 diabetes. *Front Endocrinol (Lausanne)* 2018; 9: 81.
36. Ngambenjawong C, Gustafson HH, Pun SH. Progress in tumor-associated macrophage (tam)-targeted therapeutics. *Adv Drug Deliv Rev* 2017; 114: 206–221.
 37. Pollard JW. Tumour-educated macrophages promote tumour progression and metastasis. *Nat Rev Cancer* 2004; 4: 71–78.
 38. Karnevi E, Andersson R, Rosendahl AH. Tumour-educated macrophages display a mixed polarisation and enhance pancreatic cancer cell invasion. *Immunol Cell Biol* 2014; 92: 543–552.
 39. Rodrigues Mantuano N, Stanczak MA, Oliveira IA, *et al.* Hyperglycemia enhances cancer immune evasion by inducing alternative macrophage polarization through increased o-glcacylation. *Cancer Immunol Res* 2020; 8: 1262–1272.
 40. Fraga-Silva TF, Marchetti CM, Mimura LA, *et al.* Relationship among short and long term of hypoinsulinemia-hyperglycemia, dermatophytosis, and immunobiology of mononuclear phagocytes. *Mediators Inflamm* 2015; 2015: 342345.
 41. Sun C, Sun L, Ma H, *et al.* The phenotype and functional alterations of macrophages in mice with hyperglycemia for long term. *J Cell Physiol* 2012; 227: 1670–1679.
 42. Liu HF, Zhang HJ, Hu QX, *et al.* Altered polarization, morphology, and impaired innate immunity germane to resident peritoneal macrophages in mice with long-term type 2 diabetes. *J Biomed Biotechnol* 2012; 2012: 867023.
 43. Gurusamy D, Gray JK, Pathrose P, *et al.* Myeloid-specific expression of ron receptor kinase promotes prostate tumor growth. *Cancer Res* 2013; 73: 1752–1763.
 44. Eyob H, Ekiz HA, Derosé YS, *et al.* Inhibition of ron kinase blocks conversion of micrometastases to overt metastases by boosting antitumor immunity. *Cancer Discov* 2013; 3: 751–760.
 45. Cai L, Michelakos T, Deshpande V, *et al.* Role of tumor-associated macrophages in the clinical course of pancreatic neuroendocrine tumors (pannets). *Clin Cancer Res* 2019; 25: 2644–2655.
 46. Umar A, Boland CR, Terdiman JP, *et al.* Revised bethesda guidelines for hereditary nonpolyposis colorectal cancer (lynch syndrome) and microsatellite instability. *J Natl Cancer Inst* 2004; 96: 261–268.
 47. Tan WCC, Nerurkar SN, Cai HY, *et al.* Overview of multiplex immunohistochemistry/immunofluorescence techniques in the era of cancer immunotherapy. *Cancer Commun (Lond)* 2020; 40: 135–153.

SUPPORTING INFORMATION

Additional supporting information may be found online in the Supporting Information section at the end of the article.

Figure S1 | Expression of mismatch repair proteins in various PDAC cell lines.

Table S1 | List of antibodies used in this study